

# Utilization of Logistical Regression to the Modified Sine-Gordon Model in the MST Experiment

Nizar J. Alkhateeb, Hameed K. Ebraheem, Eman M. Al-Otaibi

Department of Electronic Engineering Technology, College of Technological Studies (CTS), The Public Authority of Applied Education and Training (PAAET), Kuwait City, Kuwait  
Email: nj.alkhateeb@paaet.edu.kw

**How to cite this paper:** Alkhateeb, N.J., Ebraheem, H.K. and Al-Otaibi, E.M. (2024) Utilization of Logistical Regression to the Modified Sine-Gordon Model in the MST Experiment. *Open Journal of Modelling and Simulation*, 12, 43-58.

<https://doi.org/10.4236/ojmsi.2024.122003>

**Received:** February 22, 2024

**Accepted:** April 16, 2024

**Published:** April 19, 2024

Copyright © 2024 by author(s) and Scientific Research Publishing Inc. This work is licensed under the Creative Commons Attribution International License (CC BY 4.0).

<http://creativecommons.org/licenses/by/4.0/>



Open Access

## Abstract

In this paper, a logistical regression statistical analysis (LR) is presented for a set of variables used in experimental measurements in reversed field pinch (RFP) machines, commonly known as “slinky mode” (SM), observed to travel around the torus in Madison Symmetric Torus (MST). The LR analysis is used to utilize the modified Sine-Gordon dynamic equation model to predict with high confidence whether the slinky mode will lock or not lock when compared to the experimentally measured motion of the slinky mode. It is observed that under certain conditions, the slinky mode “locks” at or near the intersection of poloidal and/or toroidal gaps in MST. However, locked mode cease to travel around the torus; while unlocked mode keeps traveling without a change in the energy, making it hard to determine an exact set of conditions to predict locking/unlocking behaviour. The significant key model parameters determined by LR analysis are shown to improve the Sine-Gordon model’s ability to determine the locking/unlocking of magnetohydrodynamic (MHD) modes. The LR analysis of measured variables provides high confidence in anticipating locking versus unlocking of slinky mode proven by relational comparisons between simulations and the experimentally measured motion of the slinky mode in MST.

## Keywords

Madison Symmetric Torus (MST), Magnetohydrodynamic (MHD), Sine-Gordon, Toroidal, Dynamic Modelling, Reversed Field Pinch (RFP), Logistical Regression

## 1. Introduction

Plasma physics is a diverse field spanning many areas of science and technology.

A major application of plasma physics is magnetic fusion research, which has resulted in several toroidal magnetic confinement systems, such as the Madison Symmetric Torus (MST) reversed-field pinch (RFP). These toroidal magnetic confinement configurations are to date the most successful magnetic field configurations in fusion experiments. Toroidal configurations are conveniently described with a major radius  $R$  and a minor radius  $a$ .

The MST is a large toroidal reversed-field pinch experiment, in which the plasma is confined by a combination of toroidal and poloidal magnetic fields. A drawing of the MST experiment is shown in **Figure 1**. The toroidal magnetic field is produced by driving poloidal current around the conducting vacuum vessel (shell). The conducting shell contains two insulated voltage gaps. The second gap, the poloidal gap, extends the short way around the poloidal circumference of the shell to allow the poloidal magnetic field to enter.

The first gap, the toroidal gap, extends the long way (at the inside mid-plane of the torus) around the shell to allow the generation of the toroidal magnetic field inside the shell.

The poloidal magnetic field combines with the toroidal magnetic field to form a helical field, thus producing magnetic confinement of the plasma.

In MST, the plasma is formed when initially all capacitor banks are charged. Next, hydrogen gas is introduced in the vacuum chamber. Then, an electrical switch is closed to connect a capacitor bank to the toroidal-field transformer which generates the toroidal field. In consequence, a second electrical switch is closed to connect another capacitor bank to the primary winding. The discharge in the primary winding causes a current to flow in the generating a change in magnetic flux in the iron core. The change in the flux generates a toroidal electric field. Seed electrons are then injected from hot-wire filaments. The toroidal

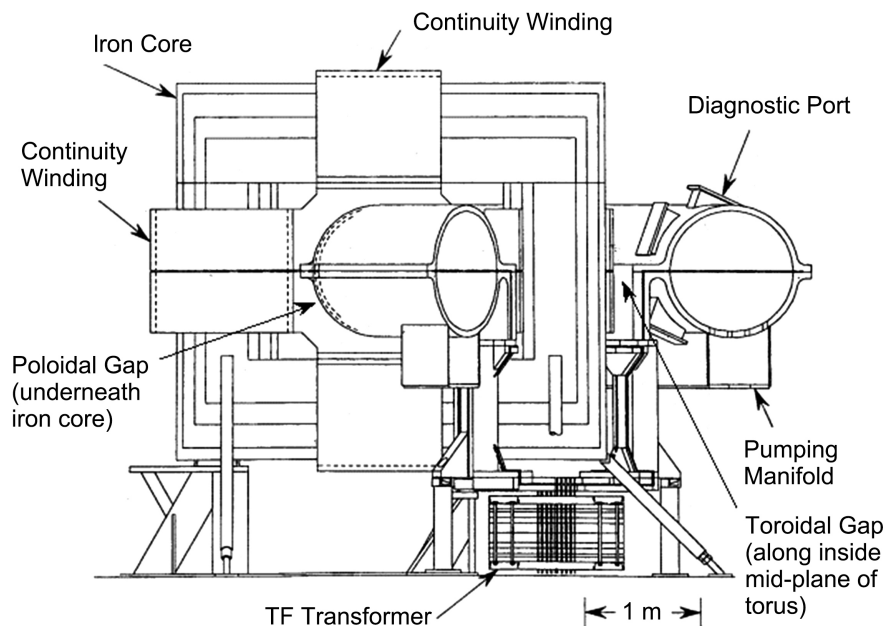


**Figure 1.** The madison symmetric torus (The cutaway view).

electric field accelerates the electrons which make collisions with the neutral gas, forming the plasma. As the plasma becomes hotter, due to ohmic heating by the toroidal current, its conductivity increases thereby ramping up the toroidal plasma current. During this time, the plasma undergoes very strong reorganization driven by MHD tearing instabilities [1]. The total toroidal flux increases while the toroidal magnetic field at the wall decreases and eventually becomes negative, (the field reversal parameter  $F$  becomes negative) forming an RFP. In MST, the reversal occurs in about 7 - 10 ms after the plasma is formed. In the standard-run condition, the current is maintained constant until about 40 ms after the discharge is started. This “flat-top” period the slinky mode is formed when most of the analysis in this paper is conducted. At 40 ms, the plasma current is ramped down and eventually the plasma cools, recombines and the shot is over around 50 ms after plasma formation as shown in **Figure 2**.

In every RFP experiment, nonlinear interactions are central to the determination of plasma behavior. In particular, the interactions between the modes lead to their phase locking and forming a fully nonlinear phenomenon known as the “slinky” mode [2] [3] [4] [5] [6]. The slinky mode is a toroidally localized helical deformation of the plasma column.

The slinky modes have been observed to lock (freeze and cease to rotate until discharge termination) at the poloidal and/or toroidal gaps due to the appearance of error fields at the gaps [3] [4] and as well as to an electromagnetic force [3] [7] [8] [9] [10].

Most experimental and theoretical studies of magnetic fluctuations, and the slinky mode in RFP experiments have relied on spatial Fourier decomposition of

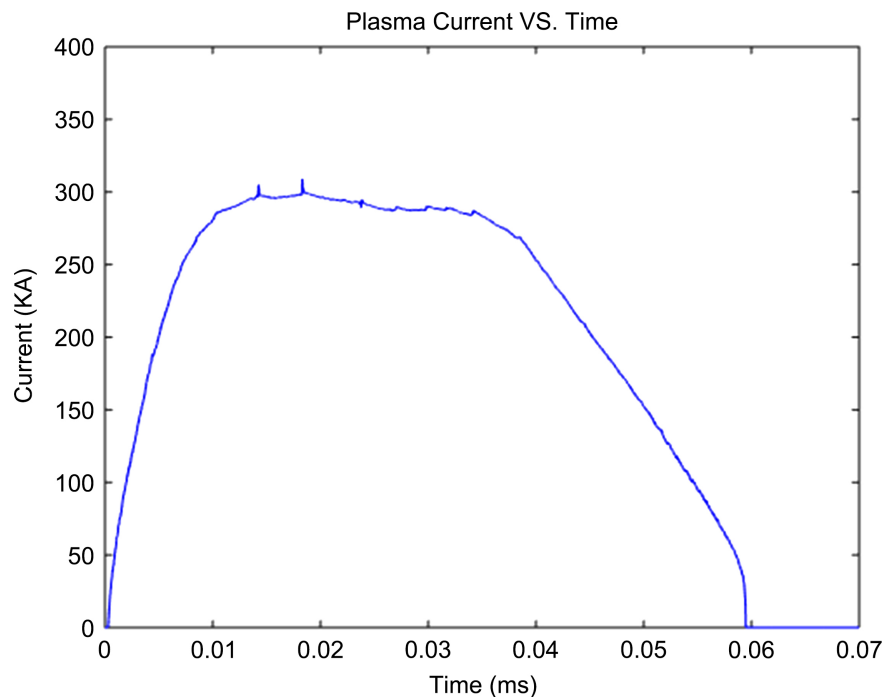


**Figure 2.** Plasma current for the entire discharge.

the fluctuations as a function of time and has been restricted to a small number of modes. Mode coupling mechanisms in RFP are due to nonlinear interaction of different Fourier MHD modes inside the plasma [2] [6] [10]. Unfortunately, Fourier methods are difficult to apply when the fundamental equations are fully nonlinear due to the appearance of additional cross-coupling terms between the Fourier modes. Moreover, linearized models in dispersive medium do not support solitary waves. In contrast, the model studied in this paper is an alternative approach addresses the full nonlinearity and does not rely on Fourier decomposition. Furthermore, the dynamics of the sine-Gordon (SG) equation cannot be completely understood using Fourier methods. The slinky-mode dynamics are coherent structures that emerge from the nonlinear SG equation that are proposed to play a central role.

This paper is a continuation of our previous paper under the title “Modeling of the mode dynamics generated by Madison Symmetric Torus machine utilizing a modified sine-Gordon equation” [11]. In [11], it was shown that the slinky mode is a kink soliton which presented a more comprehensive and more accurate model that avoided the complexities of the alternative approach utilizing Fourier spectral methods. The modified model was analyzed thoroughly in the phase plane using multiple time-scale perturbation analysis to accurately fit the experimental measurements produced by MST. Our objective in this paper is to study and analyze the parameters in the data associated with the Slinky mode from MST experiments using Logistic Regression and determine the significance of each of the seven parameters associated with experiment and utilize them in the modified Sine-Gordon dynamic model [11] [12] [13]. Furthermore, the model is solved numerically and compared to the data analyzed from MST as well as to the data detection of magnetic signals in MST experiments. In addition, we aim to emphasize the strength of each parameter and or combination of such parameters in identifying a more realistic model for causing the different phenomena for the slinky mode. The paper is organized as follows: In Section I, Experimental measurements and theoretical studies on various RFP concepts is introduced, and the formation of the mode and its mode-locking phenomena is described. In Section II, a statistical analysis of experimental measurements data to determine the significance of the various measured variables, and to determine whether the probability of locking could be predicted based on the obtained data from MST is presented. In Section III, the key significant parameters determined in section II is utilized to the dynamical equation for the MHD mode and apply numerical analysis to describe the response of the observed MHD mode in MST in accord to the experimental data.

## 2. Background

Theoretical studies [2] [5] [6] [7] [14] [15] [16] [17] and experimental measurements [3] [9] [18] [19] on mode fluctuation, magnetic field errors were performed on several RFP experiments among are MST, RFX, and TPE-RX.

In MST, dynamos are one of the most mysterious mechanism that are responsible for generating the reversed magnetic field, continually exhibit a sawtooth behavior as a function of time [20]. The sawtooth amplitude increases gradually until is reached to a critical value at which a sawtooth crash is triggered and arrests the rotation of the plasma. After the crash, the process may repeat itself.

The dominant source of field errors in MST is the poloidal gap where a high localized error field occurs [20]. The gap error field has significant effect on the plasma; hence, reducing the error field resulted in lower plasma loop voltage and plasma current enhancement.

In the TPE-RX experiment [9], it was found under certain experimental conditions that the probability of locking decreased by 25% by lowering the plasma current  $I_p$ , decreasing the plasma current rise time, and decreasing the filling pressure of the deuterium gas.

### 3. Logistic Regression Model

In this section, LR analysis of the data used to determine the significance of the variables obtained from the MST experiment is presented. The first approach was to determine whether there were any features of a discharge in MST that could be used to predict mode locking. An initial analysis of the data, obtained from several years of operation of MST, was not able to explicitly predict whether a given discharge would lock or not based on explicit values of a set of control variables. Accordingly, the analysis was modified to determine whether the probability of locking could be predicted from an analysis of the data. To determine the probability of locking, a common statistical method known as logistic regression (LR) is utilized [21] [22] [23]. The method of LR, often used for “binary” results (locking or not locking, passing or failing, etc.) to estimate the parameters of the LR model which provides a means to determine the statistical significance of any model parameters that increase or decrease the probability of locking.

To obtain a statistically significant sample of data, the LR was employed on a set of 4492 MST experimental discharges. The control (regressor) variables that were used in this analysis were  $I_p$ , the plasma current,  $V_{loop}$ , the loop voltage around the torus,  $N_{CO_2}$ , the plasma density measured with a  $CO_2$  laser,  $B_{TAVB}$ , the volume averaged toroidal field in the plasma,  $B_{TW}$ , the toroidal field on the plasma surface,  $V_{PG}$ , the voltage across the poloidal gap and  $V_{TG}$ , the voltage across the toroidal gap. The statistical analysis indicates which of the seven control variables have the strongest effects on the probability of locking. An iterative method is used to find the set of fitting parameters  $B$ 's for the predictor. The four most significant control variables determined to be  $I_p$ ,  $V_{TG}$ ,  $V_{PG}$  and  $V_{loop}$  are taking for consideration.

In **Table 1**, the values of the fitting parameters give the estimated increase or decrease in the probability of locking when the control variables are incremented by one unit. For example, for each unit of increment in  $V_{loop}$ , the probability of

**Table 1.** Coefficients of control variables obtained with logistic regression analysis.

Predictor	Fitting Parameter B	Standard Deviation	Z-value	P-value
$V_{TG}$	+0.07147	0.01177	6.07	<0.001
$V_{loop}$	-0.05329	0.006660	-8.0	<0.001
$I_p$	+0.051093	0.006946	7.36	<0.001
$V_{PG}$	+0.0333640	0.0004958	6.79	<0.001
$B_{TAVE}$	-0.029859	0.002874	-10.39	<0.001
$B_{TW}$	-0.00228	0.001651	-1.38	0.167
$N_{CO_2}$	-0.00184	0.002074	-0.89	0.375

locking will decrease by 0.05329. Similarly,  $I_p$  increases the chances of locking by 0.051093 for each unit of increment, whereas  $V_{PG}$  and  $V_{TG}$  increase the probability of locking by 0.0333640 and 0.07147, respectively. The Z and P values determine whether the control variables are statistically significant or not. In this analysis, any Z-value greater than two in magnitude and any P-value less than 0.05 in magnitude are considered statistically significant. In summary, the analysis shows that increasing  $I_p$ ,  $V_{PG}$ ,  $V_{TG}$  increases the probability of locking while increasing  $V_{loop}$  decreases the probability of locking. The variable  $B_{TAVE}$  in the preliminary analysis is not included because it is the 5th most significant variable; however, it will be examined in detail in subsequent work. Use of statistical technique does not provide a physical picture of locking phenomenon; nonetheless, it does provide significant guidance toward which variables should be included in an analysis.

#### 4. Utilization of Logistic Regression Model in the Modified Sine Gordon Equation

In this section, the key parameters obtained from Logistic Regression analysis is employed in the Modified Sine Gordon equation and compared with experimental data. The full nonlinear equation is solved numerically including all the effects dissipation  $V_{loop}$ , the driving term  $I_p$  and the presence of the poloidal voltage gap  $V_{PG}$ , of which are used to describe the behavior of the localized slinky mode in MST. The advantages of the full numerical solution are: 1) details of the shape and dynamics of the kink mode are apparent, and 2) multiple kinks dynamics or combinations of kinks and antikinks can be examined.

Recall that in [3] [7], the SM is an isolated magnetic island of finite length that travels in a helical path around the torus. The equation of motion of the SM is obtained [11] [12] [13] by summing torques acting on the mode about the magnetic axis of the main plasma, in addition to the presence of the dissipative term, the driving term and the poloidal gap term, the modified SG equation becomes

$$\phi_{tt} - \phi_{xx} + \sin \phi = \gamma - \alpha \phi_t + V_G \delta(x - x_0) \sin \phi \quad (1)$$

Equation (1) is derived and analyzed analytically in details in reference [11]. In Equation (1), it is assumed that  $\alpha$  is the normalized dissipation and related to the loop voltage  $V_{loop}$ ,  $\gamma$  is the normalized driving term and related to plasma current  $I_p$ ,  $V_G$  is the normalized intensity of the gap-slinky-mode interaction and is related to the poloidal gap voltage, and  $x_0$  is the location of the poloidal gap in the vacuum chamber. The interaction of the kink with the poloidal gap is proportional to the proximity of the kink to the gap, both axially and radially. The interactive torque is assumed to be generated by the plasma image currents in the conducting shell as described in [11].

In this paper, Equation (1) is solved numerically with all terms included. The initial conditions specified are the locations of the kink(s) and/or antikink(s) that comprise the slinky mode, and their normalized velocities. Once the initial locations and velocities are specified, the analytic solution for each of the kinks or antikinks is superimposed along a fixed distance which is assumed to be one revolution around the torus. The calculations are limited to this region to ensure numerical stability, reflecting boundary conditions are used. The representation of the derivative of the basic SG equation with respect to  $x$  is used for the following reasons: First, the derivative plot shows more clearly the details of the various interactions. Second, as the kink passes the magnetic pickup coils measure the integral of the induced current with respect to time which is similar to the derivative plot.

**Figure 3** shows the simulation of Equation (1) where all terms are included. The kink is launched with an initial velocity of 0.5. Recall that both in [11] and LR analysis, driving term which is proportional to plasma current accelerates the kink, dissipation term is proportional to loop voltage decelerates the kink at which balances kink velocity. As the kink travels towards the gap “potential hill” proportional to gap voltage will decelerate. After passing the gap, the kink will accelerate “down the hill” until it reaches steady state velocity  $U_\infty$  as defined in [11].

In **Figure 4**, the kink travels with its steady-state velocity until it nears the gap where it slows down and is bounced back because driving term cannot overcome effects of reflection.

**Figure 5** shows combinations (locking and passing the gap) of three kinks traveling with same initial velocity but at different positions. Conditions were set to achieve different phenomena. It can be seen two kinks pass through the gap while one kink locks at the gap.

In what follows the measured data obtained from MST experiment is examined and were found to be statistically significant using LR analysis. Moreover, those key variables from LR analysis of Equation (1) were utilized and simulated to replicate the data obtained from measurements for the slinky mode. In MST, the slinky mode was measured with a set of thirty-two magnetic pickup coils spaced evenly around the torus at a fixed poloidal angle [1] [3] [20]. Three

cases where the slinky mode locks, does not lock, or other phenomena that have been observed in experiments are investigated. The next goal is to show that the numerical analysis of nonlinear model accurately represents these phenomena.

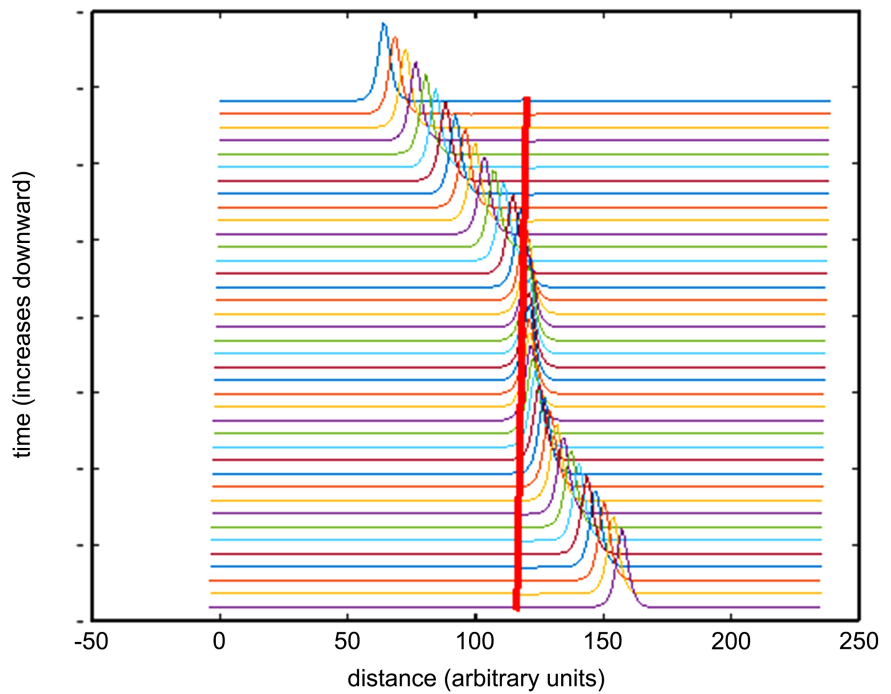


**Figure 3.** A plot of a kink that passes a potential hill (red line).  $t_{\max} = 12,000$ ,  $\alpha = 0.03$ ,  $\gamma = -0.01$ ,  $V_G = -1.35$ , and  $U = 0.3$ .

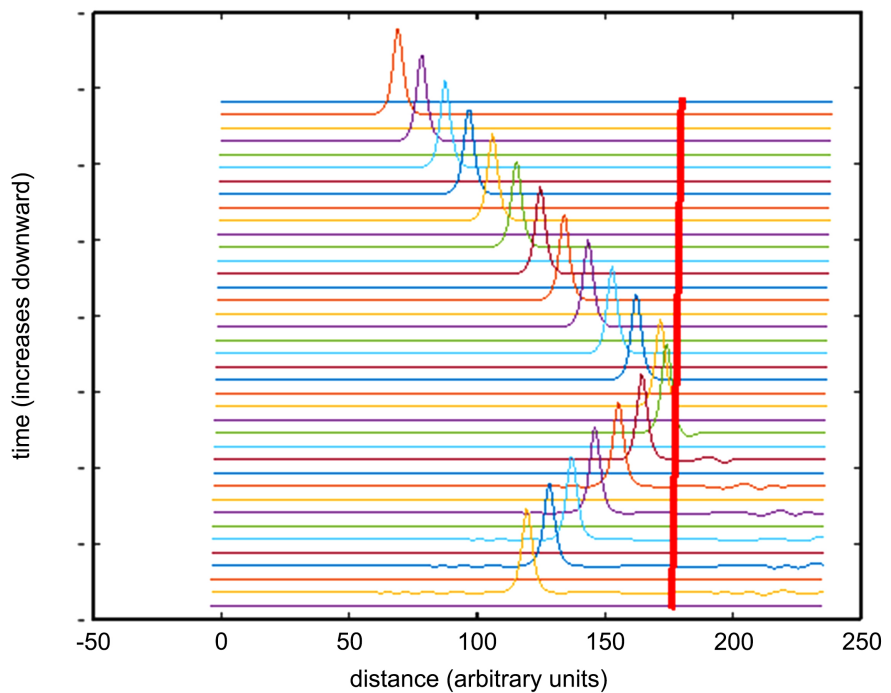


**Figure 4.** A plot of a kink that reflects back from a potential hill.  $t_{\max} = 12,000$ ,  $\alpha = 0.001$ ,  $\gamma = -0.006$ ,  $V_G = -0.0079$ , and  $U = 0.3$ .

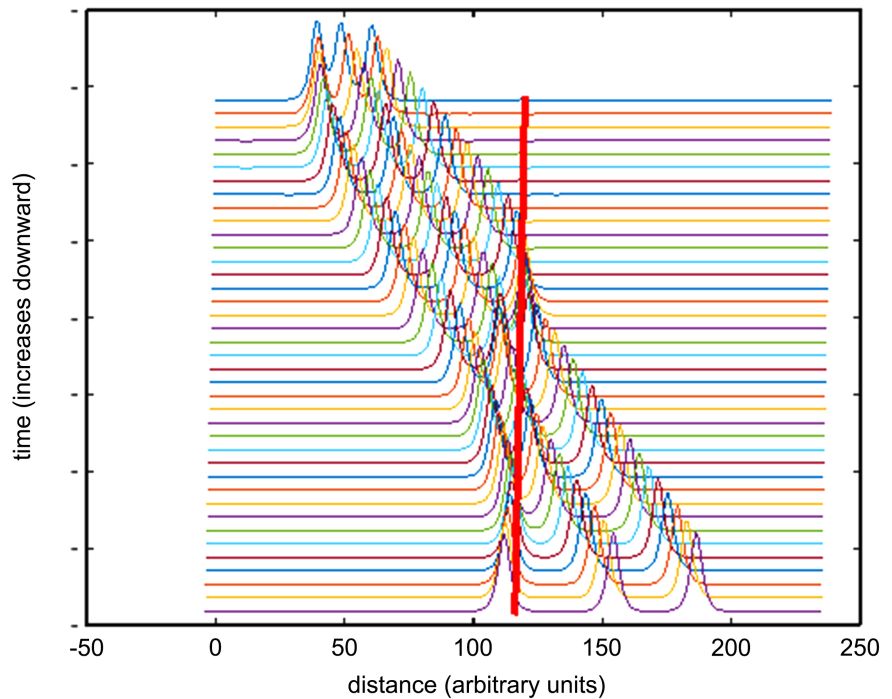


**Figure 5.** A plot of three kinks launched at separate positions toward the gap.  $t_{\max} = 12,000$ ,  $\alpha = 0.03$ ,  $\gamma = -0.01$ ,  $V_G = -1$ , and  $U = 0.3$ .

**Figure 6** shows an experimental measurement of the slinky mode at MST. In the figure, different phenomena are observed such as a slinky mode traveling in the opposite direction and bounces back (reflecting) from the poloidal gap at time nearly 20 ms, as well as, a traveling slinky mode through the gap with nearly constant velocity shown at time 20.5 ms, and an oscillating mode at the gap until it locks between the time 22 - 24 ms. It is assumed that the structure of the slinky mode shown in **Figure 6** is a chain of connected kinks, each one rotating about the magnetic axis by  $2\pi$  radians. Note that time is the horizontal axis and distance around the torus is the vertical axis.

In **Figure 7**, the effect of the gap (poloidal gap) is examined, mainly the loop voltage and the plasma current on the slinky mode for which all the three phenomena occur.

The data obtained from MST for  $I_p$ ,  $V_{loop}$ ,  $V_{PG}$  and  $V_{TG}$  are examined with their effect on the slinky mode at the instant of all three phenomena occurs are used to accurately represents the dynamical model. Recall from reference [3] [9] an increasing  $V_{loop}$ ,  $V_{PG}$ ,  $V_{TG}$  increases the probability of locking while increasing  $I_p$  decreases the probability of locking. In **Figure 7**, the significant control variables are correlated to the phenomena seen in **Figure 6** as was predicted by LR and observed in MST experiments. In **Figure 6**, prior to time 20 ms, a reflection of a rotating slinky mode is observed traveling in the opposite direction and interacts with radial magnetic field at the poloidal gap. **Figure 7** features the significant variables for the fluctuation shown in **Figure 6**, at the time of reflection, the magnitude of the voltage  $V_{PG}$  rise (13 V) across the poloidal gap which

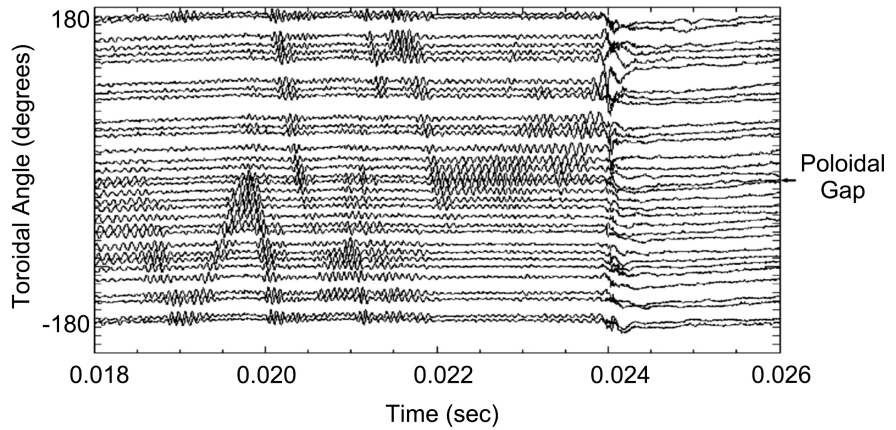


**Figure 6.** Detection of magnetic signals from the Thirty-two pickup coils in the MST experiment showing three different phenomena for the slinky modes (1) moving in the opposite direction and bounces back from the poloidal gap at time 19.75 ms, (2) Traveling and passing through the gap (non-locking) at time 20.5 ms, and (3) Traveling while oscillating at the gap until it locks.

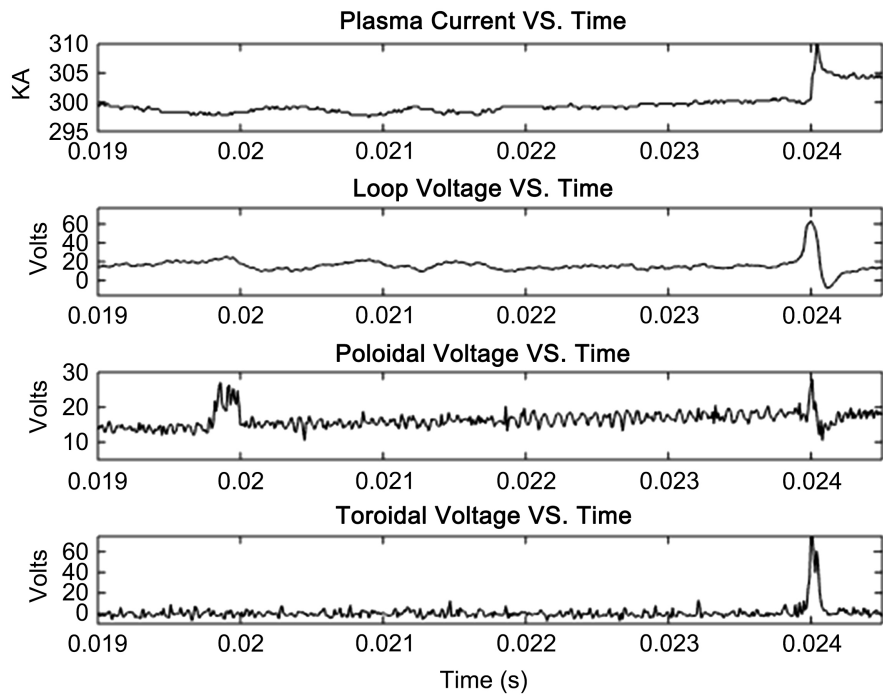


**Figure 7.** Plot for  $I_p$ ,  $V_{loop}$ ,  $V_{PG}$  and  $V_{TG}$  data obtained from the MST for the same discharge shown in Figure 6.

is proportional to the strength of the interaction at gap, while the plasma current  $I_p$  drops 3 kA, and the loop voltage  $V_{loop}$  is increased by 6 V. Moreover, at time 20.5 ms a rotating slinky mode is observed traveling with a steady state velocity thru the poloidal gap with no significant effects on LR variables. Between time 22 - 24 ms the rotating slinky mode oscillates in the vicinity of the poloidal gap until the field error rises gradually and a sawtooth crash is triggered eventually terminating the discharge in an equivalent way to LR analysis and experimental

measurements in MST. In **Figure 7**, during the time 22 - 24 ms,  $V_{pG}$  and  $I_p$  oscillates with positive slope, while  $V_{loop}$  average out to a constant.

In **Figure 8**, Equation (1) is simulated to model the bouncing kink as thirty-two samples in an equivalent way to the experimental results shown in **Figure 9**. At time prior to 20 ms, the effect of the poloidal gap on the slinky mode is examined, for example, as  $V_G$  increases on a rotating kink traveling in the opposite direction and bounces back from the gap.

**Figure 8** models a bouncing slinky mode from the gap represented in an equivalent way to the experimental results shown in **Figure 9**. The axes are the same as those in **Figure 9** and are used to compare numerical results to experimental results more easily. In **Figure 9**, at time 20.5 ms the slinky mode is traveling with steady state velocity passing thru the gap with no effects on the four LR variables due to a balance between driving and dissipation terms.

Next, the effect of the gap on slinky mode is examined precisely on which an oscillation at the gap occurs. **Figure 9** shows (at time of 22 ms) a slinky mode traveling and oscillate near the gap in MST. In **Figure 10**, the numerically calculated thirty-two sample signals is shown in an equivalent way to the experimental results shown in **Figure 9** between the time 22 - 24 ms. As an example, the observed kinks cannot pass the gap and is reflected. Due to the driving term the kinks overcome the effects of the reflection and returns to the vicinity of the gap where it is reflected again. After a number of these reflections, the kinks eventually lock to the gap. In the example, the damping coefficient is increased even though kinks do not reflect and are locked at the gap.

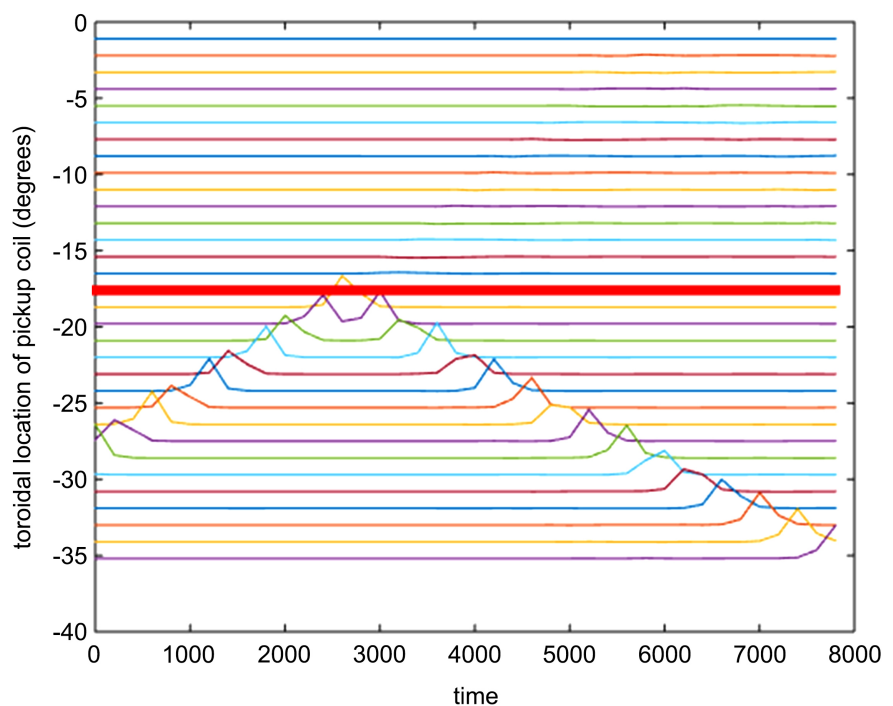


**Figure 8.** Thirty-two sampled signals for a rotating kink that bounces back from the gap.  $t_{\max} = 8000$ ,  $\alpha = 0.001$ ,  $\gamma = 0.01$ ,  $V_G = 25$ , and  $U = -0.5$ .

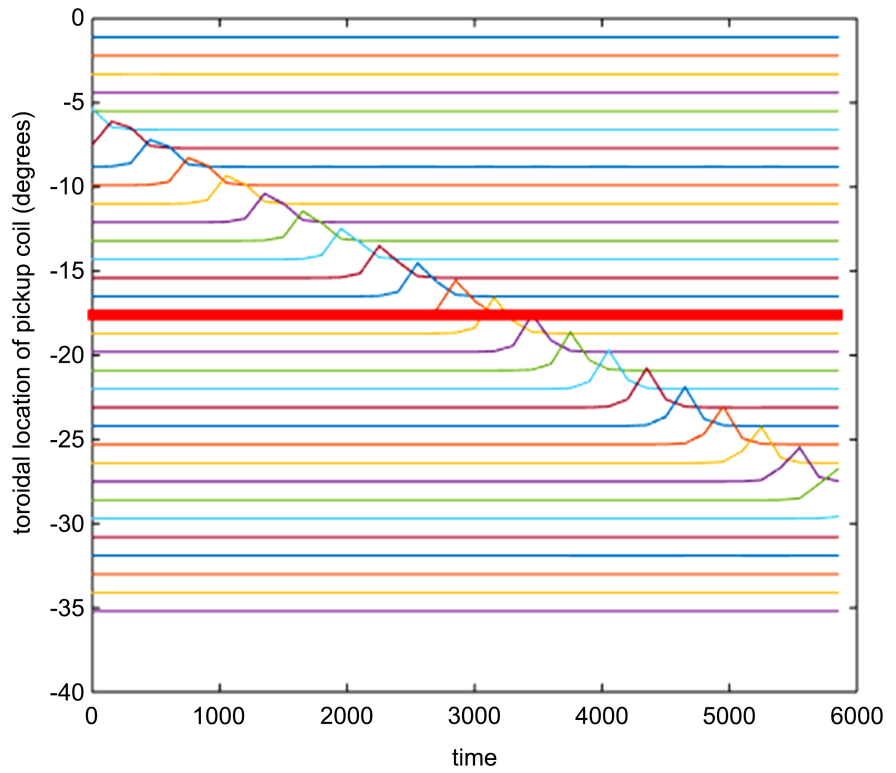


**Figure 9.** Thirty-two sampled signals for a kink passing the gap without locking.  $t_{\max} = 6000$ ,  $\alpha = 0.001$ ,  $\gamma = -0.001$ ,  $V_G = -0.005$ , and  $U = 0.5$ .

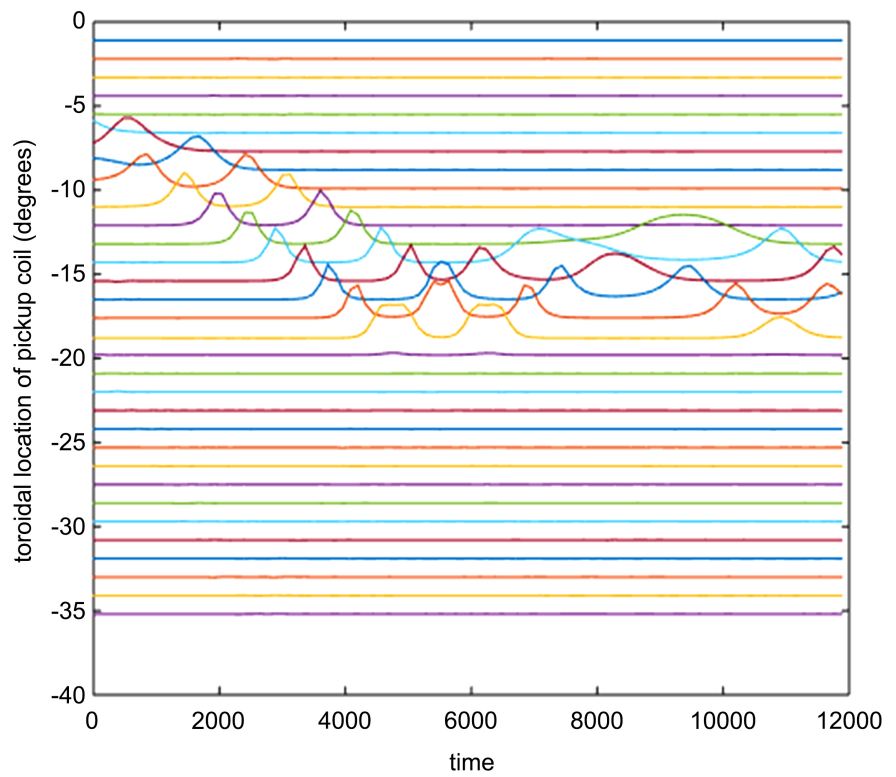


**Figure 10.** Thirty-two sampled signals for two kinks oscillating near the gap.  $t_{\max} = 12000$ ,  $\alpha = 0.008$ ,  $\gamma = -0.006$ ,  $V_G = -0.0005$ , and  $U = 0.5$ .

**Figure 11** shows the experimental results obtained in MST when the mode is locked at the gap. **Figure 12** shows the effect of the key variables obtained from LR analysis on the slinky mode locked at the gap. Prior to locking, the plasma current  $I_p$  gradually rises then averages to constant until it disappears with termination of discharge. The gap voltage  $V_{PG}$  increases slightly with positive slope, while the loop voltage  $V_{loop}$  decreases with negative slope. In **Figure 13**, the dissipation constant  $\alpha$  is increased slightly to achieve locking near the poloidal gap.

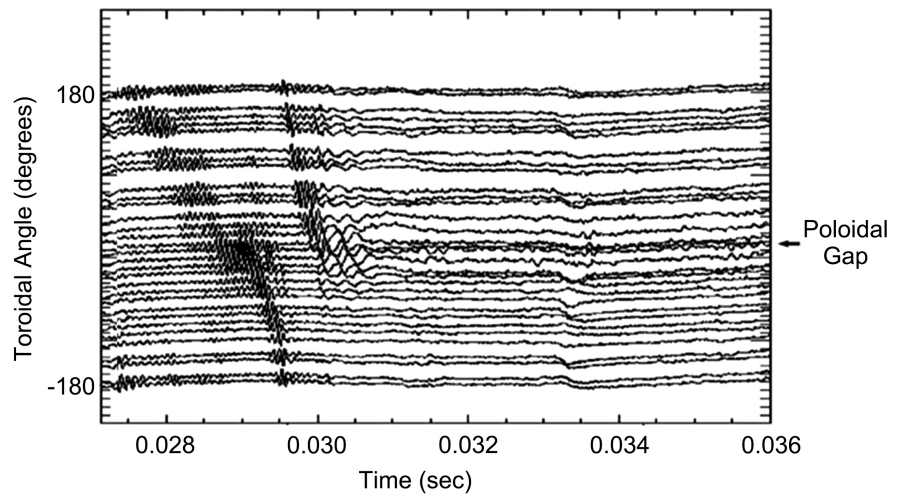


**Figure 11.** Experimental detection of locking of slinky mode in MST device. Note that the mode locks at 30 ms and disappears just slightly past the time 30.5 ms.

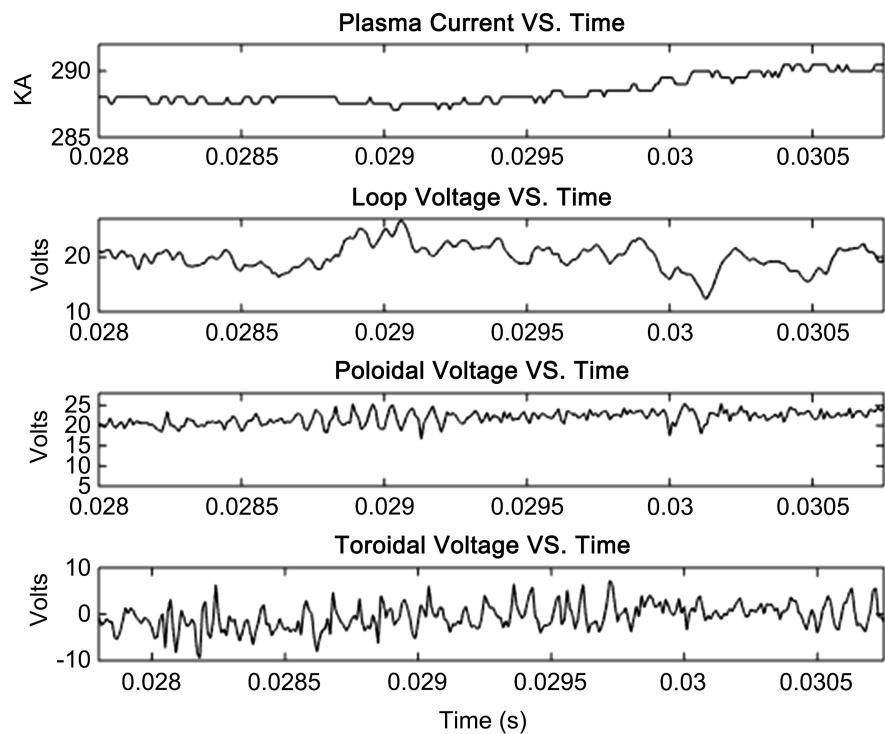


**Figure 12.** Plot for  $I_p$ ,  $V_{loop}$ ,  $V_{PG}$  and  $V_{TG}$  data results obtained in MST for the same discharge shown in **Figure 11**.

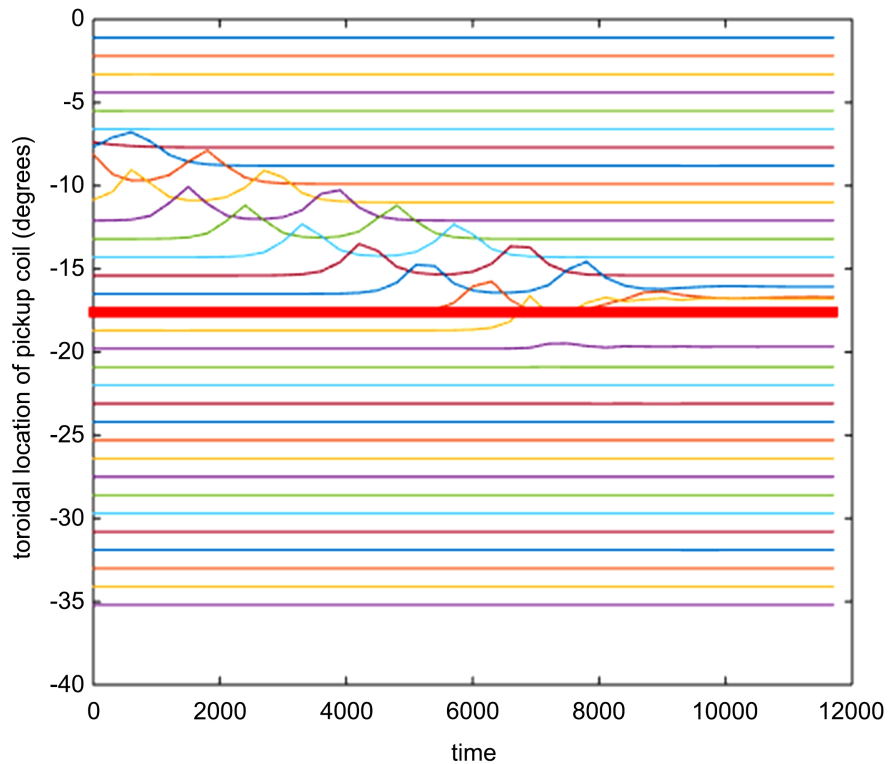


**Figure 13.** Thirty-two sampled signals for two kinks that lock just before crossing the gap at  $t_{\max} = 12,000$ ,  $\alpha = 0.1$ ,  $\gamma = -0.02$ ,  $V_G = -5$ , and  $U = 0.2$ .

## 5. Conclusions

In conclusion, this paper has demonstrated the application of logistical regression analysis (LR) to enhance the significance of key variables influencing the locking and unlocking modes in the Madison Symmetric Torus (MST) experiment. By leveraging LR, the study has identified crucial machine variables, allowing for the prediction of the high probability of locking in alignment with experimental results. The dynamical model was successfully fitted to experimental data, emphasizing the potential of LR in understanding and controlling the observed phenomena in MST.

The utilization of the modified Sine-Gordon dynamic equation model, informed by LR analysis, showcased its ability to predict the behavior of the slinky mode in the MST experiment. The study explored three distinct phenomena: a rotating slinky mode bouncing back from the poloidal gap, a mode passing through the gap without locking, and a mode oscillating near the gap until locking. The numerical simulations aligned well with experimental data, confirming the effectiveness of the LR-informed model.

Furthermore, the paper discussed the significance of key parameters, such as plasma current ( $I_p$ ), loop voltage ( $V_{loop}$ ), poloidal gap voltage ( $V_{PG}$ ), and toroidal gap voltage ( $V_{TG}$ ), in influencing the behavior of the slinky mode. The LR analysis provided insights into the impact of these variables on the probability of mode locking. The study successfully correlated LR-informed parameters with

experimental measurements, showcasing the potential for practical applications in controlling and optimizing plasma behavior in magnetic fusion research.

Overall, this research contributes to advancing our understanding of the complex dynamics in the MST experiment and provides a valuable framework for predictive modeling and control of magnetohydrodynamic modes. Future work may involve further refinement of the LR-informed model and experimental validations to enhance the accuracy and reliability of the predictive capabilities.

## Conflicts of Interest

The authors declare no conflicts of interest regarding the publication of this paper.

## References

- [1] Almagri, A.F. (2019) Private Email Communication.
- [2] Fitzpatrick, R. (1999) Formation and Locking of the “Slinky Mode” in Reversed-Field Pinches. *Physics of Plasmas*, **6**, 1168-1193. <https://doi.org/10.1063/1.873361>
- [3] Almagri, A.F., Assadi, S., Prager, S.C., Sarff, J.S. and Kerst, D.W. (1992) Locked Modes and Magnetic Field Errors in the Madison Symmetric Torus. *Physics of Fluids B: Plasma Physics*, **4**, 4080-4085. <https://doi.org/10.1063/1.860473>
- [4] Hansen, A.K., Almagri, A.F., Den Hartog, D.J., Prager, S.C. and Sarff, J.S. (1998) Locking of Multiple Resonant Mode Structures in the Reversed-Field Pinch. *Physics of Plasmas*, **5**, 2942-2946. <https://doi.org/10.1063/1.873017>
- [5] Assadi, S., Prager, S.C. and Sidikman, K.L. (1992) Measurement of Nonlinear Mode Coupling of Tearing Fluctuations. *Physical Review Letters*, **69**, 281-284. <https://doi.org/10.1103/PhysRevLett.69.281>
- [6] Hegna, C.C. (1996) Nonlinear Tearing Mode Interactions and Mode Locking in Reversed-Field Pinches. *Physics of Plasmas*, **3**, 4646-4657. <https://doi.org/10.1063/1.872033>
- [7] Hansen, A.K. (2000) Kinematics of Nonlinearly Interacting MHD Instabilities in a Plasma. Ph.D. Thesis, University of Wisconsin—Madison, Madison.
- [8] La Haye, R., Lee, P.S., Schaffer, M.J., Tamano, T. and Taylor, P.L. (1988) Magnetic Fluctuation Measurements in the Thin Resistive Shell OHTe Device Operated as a Reversed Field Pinch. *Nuclear Fusion*, **28**, Article No. 918. <https://doi.org/10.1088/0029-5515/28/5/018>
- [9] Yagi, Y., Koguchi, H., Nilsson, J.-A.B., Bolzonella, T., Zanca, P., Sekine, S., Osakabe, T. and Sakakita, H. (1999) Phase- and Wall-Locked Modes Found in a Large Reversed-Field Pinch Machine, TPE-RX. *Japanese Journal of Applied Physics*, **38**, L780. <https://doi.org/10.1143/JJAP.38.L780>
- [10] Fitzpatrick, R. and Yu, E.P. (2000) Nonlinear Dynamo Mode Dynamics in Reversed Field Pinches. *Physics of Plasmas*, **7**, 3610-3624. <https://doi.org/10.1063/1.1286990>
- [11] Ebraheem, H.K., Alkhateeb, N.J. and Sultan, E.K. (2018) Modeling of the Mode Dynamics Generated by Madison Symmetric Torus Machine Utilizing a Modified Sine-Gordon Equation. *Nonlinear Dynamics*, **93**, 1889-2001. <https://doi.org/10.1007/s11071-018-4302-2>
- [12] Ebraheem, H.K., Shohet, J.L. and Scott, A.C. (2002) Mode Locking in Reversed-Field Pinch Experiments. *Physical Review Letters*, **88**, Article ID: 235003. <https://doi.org/10.1103/PhysRevLett.88.235003>

- [13] Shohet, J.L., Barmish, B.R., Ebraheem, H.K. and Scott, A.C. (2004). The Sine-Gordon Equation in Reversed-Field Pinch Experiments. *Physics of Plasmas*, **11**, 3877-3887. <https://doi.org/10.1063/1.1763914>
- [14] White, R.L. and Fitzpatrick, R. (2015) Effect of Rotation and Velocity Shear on Tearing Layer Stability in Tokamak Plasmas. *Physics of Plasmas*, **22**, Article 102507. <https://doi.org/10.1063/1.4932994>
- [15] Fitzpatrick, R. (2015) Phase Locking of Multi-Helicity Neoclassical Tearing Modes in Tokamak Plasmas. *Physics of Plasmas*, **22**, Article ID: 042514. <https://doi.org/10.1063/1.4919030>
- [16] Xu, T., Hu, X.-W., Hu, Q.-M. and Yu, Q.-Q. (2011) Locking of Tearing Modes by the Error Field. *Chinese Physics Letters*, **28**, Article ID: 095202. <https://doi.org/10.1088/0256-307X/28/9/095202>
- [17] Tamano, T., Bard, W.D., Cheng, C., Kondoh, Y., Haye, R.J.L., Lee, P.S., Saito, M., Schaffer, M.J. and Taylor, P.L. (1987) Observation of a New Toroidally Localized Kink Mode and Its Role in Reverse-Field-Pinch Plasmas. *Physical Review Letters*, **59**, 1444-1447. <https://doi.org/10.1103/PhysRevLett.59.1444>
- [18] Sarff, J.S., Assadi, S., Almagri, A.F., Cekic, M., Den Hartog, D.J., Fiksel, G., Hokin, S.A., Ji, H., Prager, S.C., Shen, W., Sidikman, K.L. and Stoneking, M.R. (1993) Non-linear Coupling of Tearing Fluctuations in the Madison Symmetric Torus. *Physics of Fluids B: Plasma Physics*, **5**, 2540-2545. <https://doi.org/10.1063/1.860741>
- [19] Prager, S.C. and Schnack, D.D. (1989) Nonlinear Behavior of the Reversed Field Pinch with Nonideal Boundary Conditions. *Physical Review Letters*, **62**, 1504-1507. <https://doi.org/10.1103/PhysRevLett.62.1504>
- [20] Almagri, A.F. (1990) The Effects of Magnetic Field Errors on Reversed-Field Pinch Plasmas. Ph.D. Thesis, University Of Wisconsin—Madison, Madison.
- [21] Hosmer, D.W. and Lemeshow, S. (2000) Applied Logistic Regression. John Wiley & Sons, Hoboken. <https://doi.org/10.1002/0471722146>
- [22] Pregibon, D. (1981) Logistic Regression Diagnostics. *Annals of Statistics*, **9**, 705-724. <https://doi.org/10.1214/aos/1176345513>
- [23] Field, A. (2015) Discovering Statistics Using IBM SPSS Statistics. Mohn Media Mohndruck, Gütersloh.